Rare Metal Materials and Engineering
Volume 49, Issue 4, April 2020
Available online at www.rmme.ac.cn

Science Press

Cite this article as: Rare Metal Materials and Engineering, 2020, 49(4): 1177-1183.

ARTICLE

Hydrothermal Preparation of Petal-like MoS_2 and Its TG-DSC-FTIR Analysis

Zhou Jun[1,3], Wu Lei[2], Yang Rongrong[1], Zhang Qiuli[1,3], Song Yonghui[2,4], Tian Yu-hong[1,3], Lan Xinzhe[3,4]

[1] School of Chemistry and Chemical Engineering, Xi'an University of Architecture and Technology, Xi'an 710055, China; [2] School of Metallurgical Engineering, Xi'an University of Architecture and Technology, Xi'an 710055, China; [3] Shaanxi Province Metallurgical Engineering and Technology Research Centre, Xi'an 710055, China; [4] Key Laboratory of Gold and Resources of Shaanxi Province, Xi'an 710055, China

Abstract: Petal-like MoS_2 microspheres were synthesized via the hydrothermal reaction of Na_2MoO_4, $CS(NH_2)_2$, and $H_2C_2O_4$. The crystal form and morphology of MoS_2 were analyzed by XRD and SEM, and its thermogravimetric and gas precipitation properties were studied via TG-DSC-FTIR. Results indicate that product yield is influenced by the molar ratio of Mo/S, amount of reducing agent, reaction temperature, and reaction time. The crystal form of petal-like MoS_2 microspheres is hexagonal 2H-MoS_2; diameter of petal-like microspheres is 1~2 μm, and the average thickness of petal is 15~20 nm. The thermal loss process of MoS_2 can be roughly divided into two stages: transformation stage of MoS_2 and phase change stage of MoO_3, in which the first stage mainly occurs at 221.40~603.15 °C, and the second stage occurs in the temperature range of 603.15~1220 °C. MoO_2 and MoO_3 are generated in the first stage, with the thermal loss of 22.30%. A phase change of MoO_3 from solid to liquid and gas occurs in the second stage. FTIR data show that there is no SO_2 gas at 603.15 °C, which proves that MoS_2 is completely transformed before 600 °C. Compared with common MoS_2, the petal-like MoS_2 microspheres have higher reaction activity.

Key words: petal-like structure; molybdenum disulfide; hydrothermal synthesis; TG-DSC-FTIR analysis

Because of its superior lubrication, catalytic and electromagnetic properties, MoS_2 has gained wide research interest[1-3]. MoS_2 belongs to hexagonal crystal system, and its basic microstructure is Mo-S-Mo interlayer, similar to a "sandwich", in which Mo and S atoms are attached by a strong covalent bond, but S atom in interlayer relies on weak Van der Waals forces[4,5]. The microstructure and active sites of materials contribute to the microwave absorption property[6], and high specific surface and layer structure of MoS_2 as a potential material with advantageous superiority in the application of microwave absorption are widely researched[7,8].

In the past decade, nano-MoS_2 with diverse morphologies can be successfully prepared via ultrasonic chemical synthesis, gas reaction, thermal decomposition, and hydrothermal synthesis. Among them, hydrothermal synthesis is considered as the most promising approach because of its simple operation, low cost, high efficiency, and mild reaction conditions[9,10]. Qiao et al[11] successfully synthesized uniform hierarchical MoS_2 microspheres via facile hydrothermal method with the aid of nonionic surfactant polyethylene glycol. The results indicated that as-prepared MoS_2 microspheres show superior performance in the removal of methylene blue from aqueous solution and can be used as an efficient, robust and recyclable adsorbent in water treatment application. Tang et al[12] also prepared nano-MoS_2 assisted by hydrothermal method to study tribological properties, and results show that the base oil with 2.0 wt% as-prepared MoS_2 has a better anti-wear ability.

TG-DSC is a technique to analyze thermal loss and energy

Received date: April 15, 2019
Foundation item: National Natural Science Foundation of China (51774227); Natural Science Foundation Program of Shaanxi Province for Key Basic Research (2017ZDJC-33); Natural Science Foundation Program of Shaanxi Province for Joint Fund Project (2019JLP-17); International Scientific and Technological Cooperation Project of Shaanxi Province (2019KW-049)
Corresponding author: Zhou Jun, Ph. D., Professor, School of Chemistry and Chemical Engineering, Xi'an University of Architecture and Technology, Xi'an 710055, P. R. China, Tel: 0086-29-82201248, E-mail: xazhoujun@126.com

change using thermogravimetric analysis (TG/TGA) and differential scanning calorimetry (DSC), which is widely used to investigate the thermal behavior during combustion process. TG-DSC coupled with Fourier transform infrared spectroscopy (FTIR) can continuously detect the real-time mass loss and gas evolution rule during TG process[13]. Malgorzata et al[14] made it possible to determine the composition of shale rocks using thermal methods and Fourier transform infrared spectroscopy, and divided thermal decomposition into three sections to study the thermal loss rule. Ou Yapeng et al[15] investigated the thermal decomposition behavior of hydroxyl terminated polyether (HTPE) based polyurethanes (PUs) by DSC-TG-MS-FTIR. The results show that the decomposition mechanism of HTPE based PU is a two-step process after endothermic melting and the influence mechanism of energetic and inert plasticizer on decomposition of HTPE based PU is different. Grochowicz et al[16] investigated the thermal properties of polymeric microspheres and their modification by drug molecules and silica gel counterparts under oxidative atmosphere using TG-DSC-FTIR methods, and it is discovered that the thermal degradation of polymeric microspheres has at least four exothermic stages but modified polymeric microspheres decompose in only two stages.

As a promising transition metal compound, MoS_2 with high specific surface and layer structure has been widely used in many fields[17-19]. For example, Yang et al[20] prepared MoS_2 nanoparticles via a facile hydrothermal method, and doped them onto In_2O_3 hollow microtubes for NO_2 gas sensing. Although the sensing performance is excellent, severe agglomeration and bad dispersion restrict the performance improvement. However, the research on thermal stability of above MoS_2 has not received much attention, especially in catalytic application. In this study, the petal-like MoS_2 was prepared by hydrothermal method and applied as the microwave pyrolysis catalyst. The effects of Mo/S ratio, proportion of reducing agent, reaction temperature and reaction time on petal-like MoS_2 yield were studied, and the optimal combination conditions were also acquired using single factor experiments. Meanwhile, the thermostability of petal-like MoS_2 was further evaluated through TG-DSC-FTIR methods to reveal the mass and heat changes of MoS_2 in air atmosphere at different temperatures.

1 Experiment

The reagents in preparation experiment were all analytical reagents, purchased from Sinopharm Group of China. All reagents were used without further purification.

According to a certain molar ratio, sodium molybdate and oxalic acid were uniformly mixed with deionized water in PTEF liner and then thiourea was added in proportion. After fully stirring, hydrothermal reaction was conducted in vacuum-drying at required reaction temperature and time. Product was separated by high-speed centrifuge, and then repeatedly washed by deionized water and absolute ethyl alcohol three or four times. After drying at 60 °C for 12 h, product was calcined for 2 h at high temperatures (400~900 °C) in electric tube furnace with argon as protective gas. At last, black powder products were collected and weighted. The technological process of MoS_2 preparation is described in Fig.1. 5 mg MoS_2 sample was put into porcelain crucible on a balance bracket, and heated to 1200 °C at the heating rate of 10 °C/min in air atmosphere (DSC-TGA, STA409PC). Meanwhile, thermal loss data were automatically calculated, and gas composition was detected by FTIR.

X-ray diffraction technology was employed to detect the crystal form using a NaI (TI) detector and Cu Kα radiation at 40 kV and 30 mA (XRD, Type-7000). The scanning range of 2θ was between 5° and 80° at a rate of 0.02 °C/s. Scanning electron microscopy with energy dispersive spectrometry

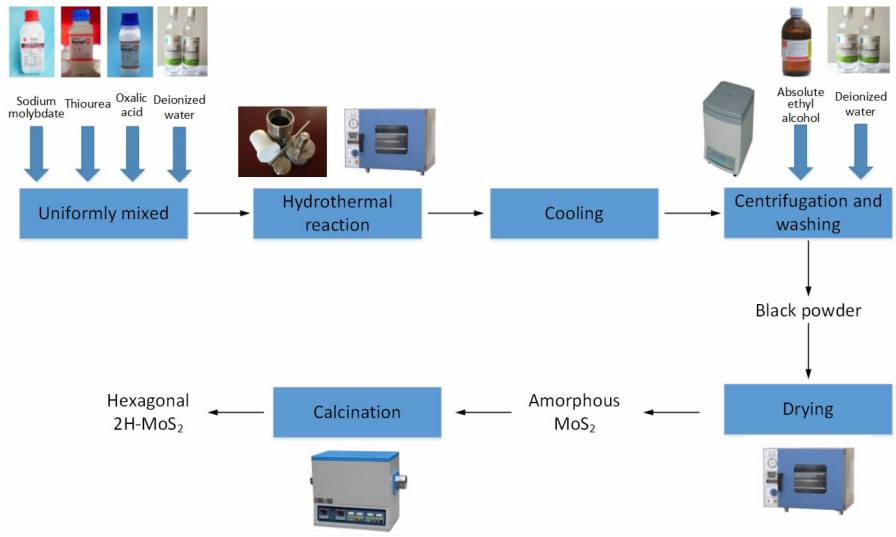

Fig.1 Technological process of MoS_2 preparation

(SEM-EDS, JSM-6360LV) was used to analyze the micromorphology and elementary composition at a resolution of 1.6 nm and accelerating voltage of 30 kV. Gas precipitation rule was investigated by Fourier transform infrared spectrometer (FT-IR, VERTEX70), and the spectra were recorded with various indices between 4000 cm^{-1} and 500 cm^{-1} by co-adding 32 scans at a resolution of 4 cm^{-1}.

2 Results and Discussion

2.1 Yield of product

According to different experimental conditions, various yields of product are obtained, and test numbers corresponding to various yields are signed in Fig.2. The yields of MoS_2 with different Mo and S atom ratios clearly demonstrate that the yield increases with adding more $CS(NH_2)_2$, but when the molar ratio of Na_2MoO_4:$CS(NH_2)_2$ is lower than 1:5, the yield is no longer increased, as shown in Fig.2a. Due to the lack of $CS(NH_2)_2$, the H_2S produced from hydrolysis reaction of thiourea is less, which leads to system partial pressure reduction. With the double effects of less H_2S content and lower partial pressure, the concentration of H_2S is reduced, and the sulfidation will certainly be weaken to decrease the yield of MoS_2 in the same reaction time. Another reason for reduced yield of MoS_2 is by-product MoO_2 generated. When the molar ratio of Na_2MoO_4:$CS(NH_2)_2$ is 1:5, the maximum yield of MoS_2 is about 85 wt%. The yields of MoS_2 with different $H_2C_2O_4$ additions are shown in Fig.2b. As the molar ratio of $H_2C_2O_4$:Na_2MoO_4 increases from 0.7:1 to 1:1, the yield of MoS_2 approximately is increased by 35 wt%. After then, the yields decrease slightly with the increase of $H_2C_2O_4$:Na_2MoO_4. When the molar ratio of $H_2C_2O_4$:Na_2MoO_4 is 1:1, the Na_2MoO_4 is completely reduced, which closely matches to the calculation amount of $H_2C_2O_4$. As shown in Eq.(1~3), $H_2C_2O_4$ and H_2S are the reducing agent in reaction process. When adding more $H_2C_2O_4$, excessive H^+ may reduce MoO_2 so the yield of MoS_2 goes down.

$$Na_2MoO_4 + H_2C_2O_4 \rightarrow MoO_2 + Na_2CO_3 + H_2O + CO_2(g) \quad (1)$$

$$CS(NH_2)_2 + 2H_2O \rightarrow 2NH_3(g) + CO_2(g) + H_2S\ (g) \quad (2)$$

$$MoO_2 + 2H_2S \rightarrow MoS_2 + 2H_2O \quad (3)$$

The reaction temperature deeply affects the yield of MoS_2, as shown in Fig.2c, when the temperature increases by 40 °C, the yield improves by 75 wt%. The product yield increases to 85 wt% at 220 °C, but when temperature increases to 240 °C, the yield decreases slightly. The variation of product yield is caused by two main reasons: one is high reaction temperature that makes reaction rate constant higher and accelerates positive reaction of Eq.(3), the other is high pressure caused by solvent evaporation that results in high diffusion velocity and enhanced hydrothermal reaction. Fig.2d shows that the hydrothermal reaction needs enough time to obtain high product yield. Once the reaction time is more than 8 h, the product yield improves to 80 wt%, and the maximum yield of 85 wt% is acquired after

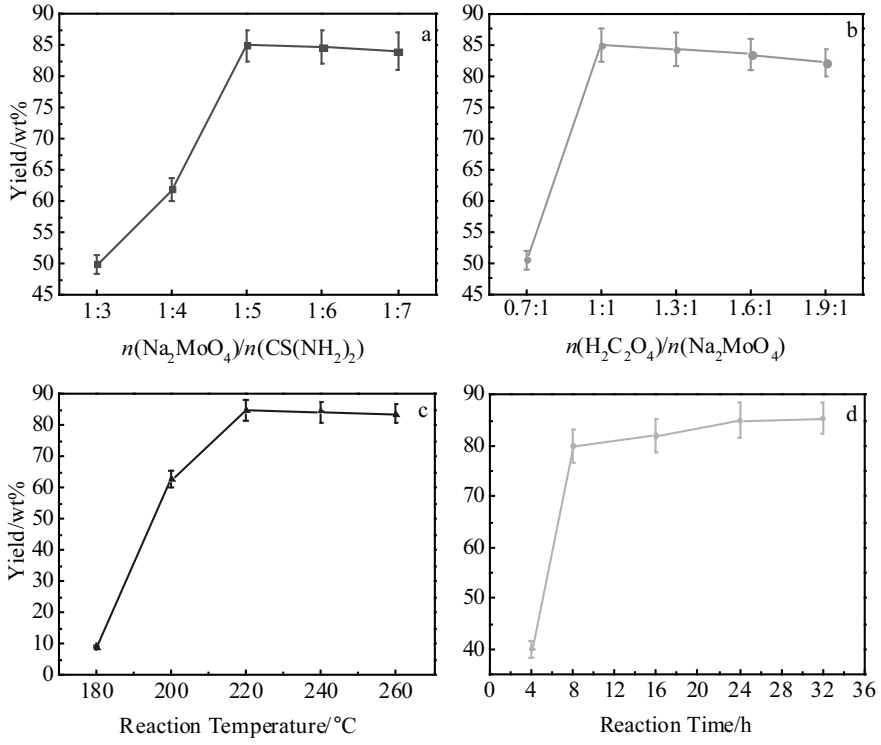

Fig.2 Yields of product in different single factor experiments: (a) molar ratio of Na_2MoO_4:$CS(NH_2)_2$, (b) molar ratio of $H_2C_2O_4$:Na_2MoO_4, (c) reaction temperature, and (d) reaction time

reaction time of 24 h. The single factor experimental results show that the optimum reaction conditions are as follows: the molar ratio of Na_2MoO_4:$CS(NH_2)_2$ is 1:5, the molar ratio of $H_2C_2O_4$:Na_2MoO_4 is 1:1, and the reaction temperature and reaction time are 220 °C and 24 h, respectively, and then the maximum product yield can be achieved.

2.2 Structure and morphology

Fig.3 shows the XRD patterns of petal-like MoS_2 microspheres obtained via hydrothermal experiment. The characteristic diffraction peaks at 13.1°, 29.2°, 33.5°, 39.8°, 44.2°, 49.15°, 58.23° and 61.6° correspond to crystal indexes of (002), (004), (100), (103), (006), (005), (110) and (008), respectively. Compared with the standard card of hexagonal MoS_2 (JCPDS No.37-1492), the XRD results confirm that petal-like MoS_2 is pure hexagonal 2H-MoS_2 and the lattice constants of *a* and *c* calculated are 0.316 16 and 1.229 58 nm, respectively. The diffraction peak of (002) is high and sharp to certify the good stackable layered structure of petal-like MoS_2, which can be verified by SEM images.

The morphology of as-prepared MoS_2 is observed by SEM with different magnifications, and the elemental composition of marked position in Fig.4c is detected by EDS. As shown in Fig.4a and Fig.4b, the shape of particles nearly likes globular with an average diameter of 1~2 μm, and particles aggregate into dense clumps. SEM image (Fig.4c) reveals that the petal-like MoS_2 microspheres are self-assembled by plicate nanosheets that have a thickness of 15~20 nm. The plicate nanosheets provide more active sites in high energy field to improve reaction activity. The EDS spectrum of nanosheet shows that the main elements are Mo and S in marked position, and no other element is observed. The result of quantitative analysis for peak area shows that the atom ratio of Mo:S is about 1.94:1, which is very close to atom stoichiometric ratio of MoS_2.

2.3 TG-DSC-FTIR

The thermal behavior of MoS_2 during oxidation is investigated at 10 °C/min under air atmosphere by TGA and the result curves are shown in Fig.5. There are four curves representing mass change (TG), mass loss rate (DTG), heat variation (DSC) and temperature change (Tem) in Fig.5.

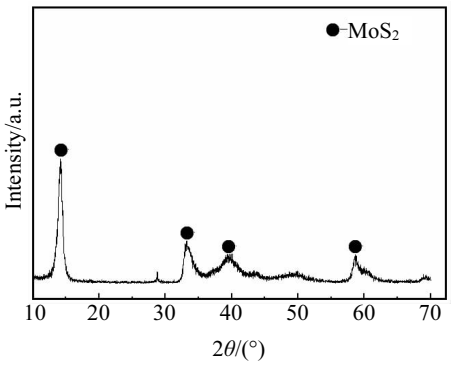

Fig.3 XRD pattern of petal-like MoS_2

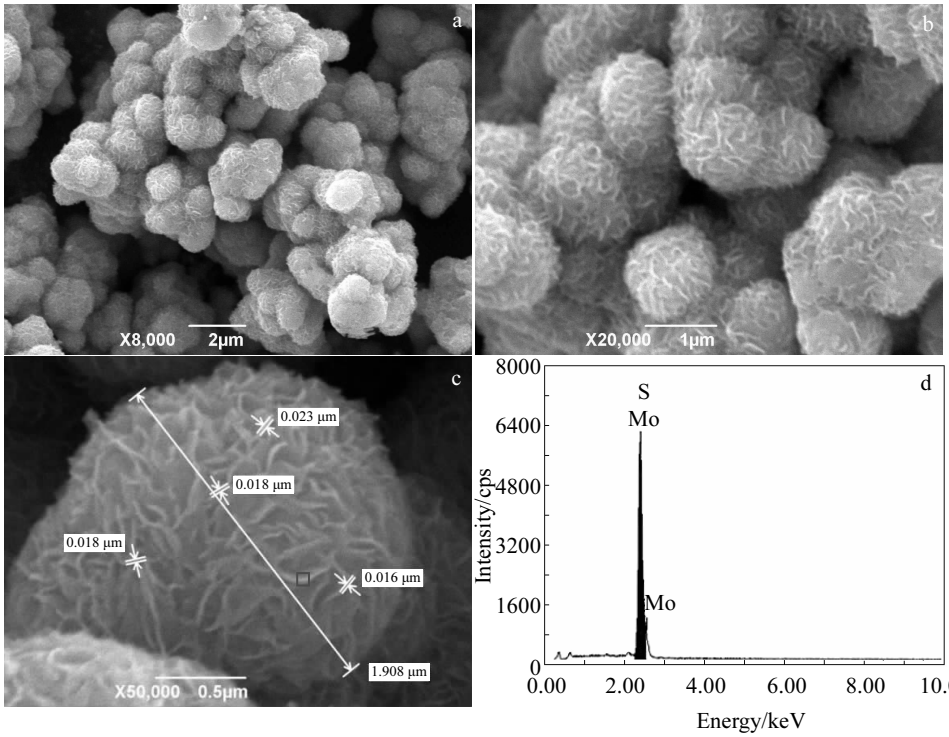

Fig.4 SEM images (a~c) and EDS spectrum of the position marked in Fig.4c (d) of petal-like MoS_2

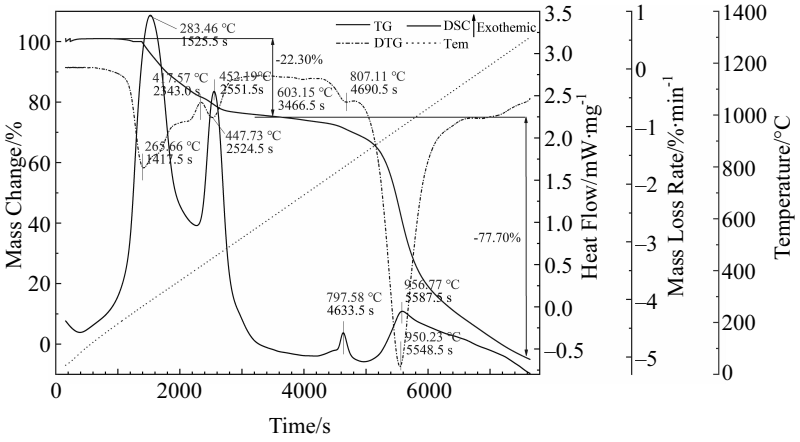

Fig.5 TG-DSC curves of petal-like MoS_2

It can be seen from TG curve that the mass loss begins at about 221.40 °C, and total loss ends at 1200 °C. The mass change can be roughly divided into two stages. One is transformation stage of MoS_2, which begins at about 221.40 °C and ends at 603.15 °C. MoS_2 is completely oxidized to MoO_2 and MoO_3 with a mass loss of 22.30%. The other is phase change stage of MoO_3, during which MoO_3 solid transforms into gas by high temperature. If all MoS_2 is oxidized to MoO_2 or MoO_3, the mass loss decreases 20% or 10% by calculation of reaction equation (Eq.(5) and Eq.(6)). Hence, the mass loss of 22.30% indicates that easily oxidized impurities must exist and MoS_2 must be oxidized to MoO_2 and MoO_3. Although the boiling point of MoO_3 is 1155 °C, MoO_3 begins to volatilize before 600 °C[21]. As shown in the DTG curve, the mass loss rate peaks appear at the temperatures of 265.66, 447.73, 807.11 and 950.23 °C, which indicate much mass reduction at corresponding temperatures, and the maximum rate is 5.2%/min at the temperature of 905.23 °C, which is caused by chemical reaction and phase change. The mass loss rate hardly alters and is close to zero in the range of 500 °C to 700 °C, which may be due to the fact that the generation rate of MoO_3 via Eq.(6) is close to the oxidized rate of impurities.

$$MoS_2 + 3O_2 \rightarrow MoO_2 + 2SO_2 \quad (4)$$

$$MoS_2 + \frac{7}{2}O_2 \rightarrow MoO_3 + 2SO_2 \quad (5)$$

$$MoO_2 + \frac{1}{2}O_2 \rightarrow MoO_3 \quad (6)$$

DSC curve demonstrates that four exothermic peaks correspond to mass loss rate peaks. Because of oxidization of air, heat starts to release at the temperature of 221.40 °C, along with the generation of MoO_2, and when the reaction temperature reaches 283.46 °C, MoS_2 is further transformed, releasing a large amount of heat. This is why the first exothermic peak appears at temperature of 283.46 °C. With rising the temperature, MoO_2 is converted to MoO_3 and heat is released meantime, which causes the second exothermic peak at 452.19 °C. The third and fourth exothermic peaks corresponding to 797.58 and 956.77 °C may be caused by crystal modification at high temperature to reduce energy absorption. Due to phase change of MoO_3, the value of DSC is less than zero, and thermal behavior is endothermic. Compared with common MoS_2[22], temperature of the first exothermic peak is lower, which indicates that the bridge of Mo and S more easily breaks at low temperature. Therefore, the petal-like MoS_2 microsphere acts out high reaction activity. The temperature rising curve shows that it takes about 7200 s to rise temperature from 25 °C to 1200 °C at a heating rate of 10 °C/min.

The 3D FTIR spectra of gaseous products are depicted in Fig.6, and the segmental patterns at key temperatures are analyzed in detail. As shown in the spectra, six absorption peaks can be obviously found around 3750, 2350, 2100, 1540, 1380, and 1195 cm^{-1}. According to the IR absorption peaks of functional groups[23], the peak at 3750 cm^{-1} belongs to the stretching vibration of water vapor that may be carried in air. A remote possible is nitric oxide represented by the peak at 3750 cm^{-1} that is generated by nitrogen and oxygen with a metal molybdenic catalyst in high energy[24,25]. The absorption peaks at 2350, 2100 and 1540 cm^{-1} are carbon dioxide, carbon oxide and organic compound stretching vibration, respectively. This is because petal-like MoS_2 with developed surface structure and high specific surface area adsorbs the initial reactants, and then reactants are oxidized to carbon dioxide, carbon oxide and aromatic. The peaks between 1195 and 1380 cm^{-1} show sulfur dioxide stretching vibration. It is verified that MoS_2 is oxidized to molybdenum oxide and sulfur dioxide, as shown in Eq.(4) and Eq.(5).

The peak intensity is proportional to the evolved gas concentration according to the Beer-Lambert law[26]. So, various gas concentrations at different temperatures are calculated via the absorption fluctuation, and the effect of temperature on the precipitation rule of gas is analyzed in Fig.7. Sulfur dioxide is

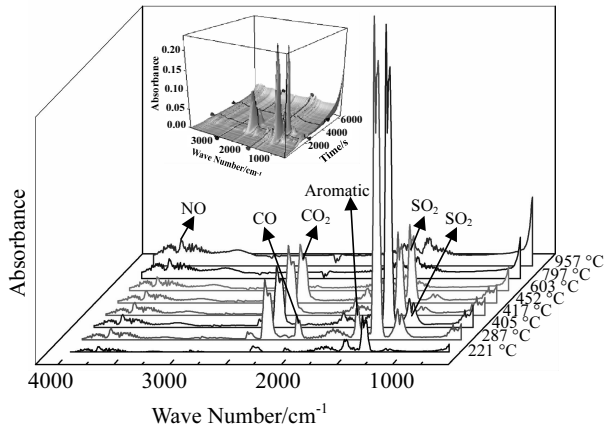

Fig.6 FT-IR spectra of gas at different temperatures

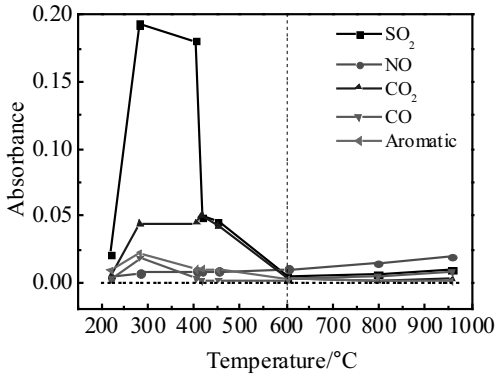

Fig.7 Gases precipitation under different temperatures

the main gas product, and begins to release at 221.40 °C. Yield of sulfur dioxide firstly increases and then decreases to zero with the increase of temperature before 603.15 °C, and the maximum yield is gained at 283.46 °C. This is consistent with the results of TG and DTG curves. The yield of carbon dioxide is only second to that of sulfur dioxide, and the change rule is similar, whose maximum yield is gained at 417.57 °C. There is little variation in yield of water vapor from beginning to end, which confirms that the moisture comes from air. When the heating temperature reaches about 603.15 °C, the main gaseous products are no longer generated, and the yields are near to zero. This fully proves complete transformation of MoS_2.

3 Conclusions

1) Petal-like MoS_2 is prepared by hydrothermal method. The maximum product yield of 85 wt% is obtained under the optimum conditions: the molar ratio of Na_2MoO_4:$CS(NH_2)_2$ is 1:5, the molar ratio of $H_2C_2O_4$:Na_2MoO_4 is 1:1, and the reaction temperature and reaction time are 220 °C and 24 h, respectively.

2) The crystal form of petal-like MoS_2 microspheres is hexagonal 2H-MoS_2; diameter of petal-like microspheres is 1~2 μm and average thickness of plicate nanosheets is 15~20 nm.

3) Thermal loss process of MoS_2 can be roughly divided into two stages: transformation stage of MoS_2 (221.40~603.15 °C) and phase change stage of MoO_3 (603.15~1200 °C), and the mass loss rate is 22.30% in the first stage along with the formation of MoO_2 and MoO_3. The DSC results show that the petal-like MoS_2 microsphere acts out high reaction activity, and crystal structure of MoO_3 changes at 797.58 and 956.77 °C. The FTIR indicates that the main released gas is sulfur dioxide, water vapor or nitric oxide, carbon oxides and organic, and MoS_2 is completely transformed before 603.15 °C.

References

1 Zhang Weidong, Zhang Xue, Wu Hongjing *et al. Journal of Alloys and Compounds*[J], 2018, 751: 34
2 Li Meijuan, Shen Shuyi, Luo Guoqiang *et al*. *Chinese Journal of Inorganic Chemistry*[J], 2017, 33(9): 1521
3 Zhou Jun, Chen Yunfei, Wu Lei *et al*. *Energy & Fuels*[J], 2017, 31: 6895
4 Sun Yuan, Zhong Wei, Wang Yuanqi *et al*. *ACS Applied Materials & Interfaces*[J], 2017, 9(39): 34 243
5 Zhang Yajie, Zeng Wen, Li Yanqiong. *Journal of Alloys and Compounds*[J], 2018, 749: 355
6 Li Huifeng, Huang Yunhua, Sun Genban *et al*. *The Journal of Physical Chemistry C*[J], 2010, 114(22): 10 088
7 Zhang Xiaojuan, Wang Shanwen, Wang Guangsheng *et al*. *RSC Advances*[J], 2017, 7: 22 454
8 Zhang Xiaojuan, Li Sheng, Wang Shanwen *et al*. *The Journal of Physical Chemistry C*[J], 2016, 120(38): 22 019
9 Bai Lizhong, Wang Yanhui, Zhang Zengyi *et al*. *Materials Review B*[J], 2017, 31(8): 12
10 Fu Chongyuan, Song Xing, Tao Shen *et al*. *Acta Physica Sinica*[J], 2015, 64(1): 16 102
11 Qiao Xiuqing, Hu Fuchao, Hou Dongfang *et al*. *Materials Letter*[J], 2016, 169: 241
12 Tang Guogang, Zhang Jing, Liu Changchao *et al*. *Ceramics International*[J], 2014, 40: 11 575
13 Musellim Ece, Mudassir Hussain Tahir, Muhammad Sajjad Ahmad *et al*. *Applied Thermal Engineering*[J], 2018, 137: 54
14 Malgorzata Labus, Malogorzata Lempart. *Journal of Petroleum Science and Engineering*[J], 2018, 161: 311
15 Ou Yapeng, Sun Yalun, Guo Xueyong *et al*. *Journal of Analytical and Applied Pyrolysis*[J], 2018, 132: 94
16 Grochowicz Marta, Agnierzka Kierys. *Polymer Degradation and Stability*[J], 2017, 138: 151
17 Bao Jun, Zeng Xiaofei, Huang Xiejun *et al*. *Journal of Material Science*[J], 2019, 54: 14 845
18 Muharrem Acerce, Damien Voiry, Manish Chhowalla. *Nature Nanotechnology*[J], 2015, 10: 313
19 Zhou Jun, Wu Lei, Liang Kun *et al*. *Journal of Analytical and*

Applied Pyrolysis[J], 2018, 134: 580
20 Yang Zhimin, Zhang Dongzhi, Chen Haonan. *Sensors and Actuators B: Chemical*[J], 2019, 300: 127 037
21 Guo Peimin, Zhao Pei, Li Zhengbang. *Special Steel*[J], 2006, 27(6): 30 (in Chinese)
22 Tian Yumei. *Thesis for Doctorate*[D]. Jilin: Jilin University, 2006 (in Chinese)
23 Gao Qiankun. *Thesis for Doctorate*[D]. Beijing: University of Science and Technology of China, 2017 (in Chinese)
24 Zheng Dongyun. *Thesis for Doctorate*[D]. Wuhan: Wuhan University, 2010 (in Chinese)
25 Zhang Jie. *Anhui Chemical Industry*[J], 2016, 42(4): 46 (in Chinese)
26 Gao Ningbo, Li Aimin, Quan Cui *et al. Journal of Analytical of Applied Pyrolysis*[J], 2013, 100: 26

水热法制备球花状 MoS_2 及其热红联用分析

周　军[1,3]，吴　雷[2]，杨茸茸[1]，张秋利[1,3]，宋永辉[2,4]，田宇红[1,3]，兰新哲[3,4]

(1. 西安建筑科技大学 化学与化工学院，陕西 西安 710055)

(2. 西安建筑科技大学 冶金工程学院，陕西 西安 710055)

(3. 陕西省冶金工程技术研究中心，陕西 西安 710055)

(4. 陕西省黄金与资源重点实验室，陕西 西安 710055)

摘　要：以 Na_2MoO_4 为钼源，$CS(NH_2)_2$ 为硫源，$H_2C_2O_4$ 为还原剂，采用水热合成法制备了球花状 MoS_2 微球，并利用 XRD、SEM-EDS 和 TG-DSC-FTIR 等分析手段对其晶型、微观形貌、热性能等进行分析。结果表明：Mo/S 摩尔比、还原剂添加量、反应温度和反应时间均对产率产生影响。球花状微球为纯净的六角 2H-MoS_2，微球直径为 1~2 μm，微球上球花厚度为 15~20 nm。球花状 MoS_2 微球热损失大致可以分为 2 个阶段：MoS_2 转化阶段（温度区间为 221.40~603.15 ℃）和 MoO_3 相变阶段（温度区间为 603.15~1220 ℃）。转化阶段 MoS_2 转化为 MoO_2 和 MoO_3，质量损失为 22.3%；相变阶段主要是发生了固相 MoO_3 转变为液相和气相的相变反应。FTIR 结果表明，SO_2 气体在 603.15 ℃之前全部析出，证明了 MoS_2 在 600 ℃左右完全转化。与常规 MoS_2 相比，球花状 MoS_2 微球表现出更高的活性。

关键词：球花结构；二硫化钼；水热合成；热重分析；红外分析

作者简介：周　军，男，1977 年生，博士，教授，西安建筑科技大学化学与化工学院，陕西 西安 710055，电话：029-82201248，E-mail: xazhoujun@126.com